INVESTIGATIONS OF FAILURE BEHAVIOUR OF FLAWED STEEL SPECIMENS WITH ELECTRON BEAM WELDS (EBW)

A.Bajric[1], W.Brocks[2], W. Dahl[1], J. Heyer[3] and P. Langenberg[4]
[1]Department of Ferrous Metallurgy, Aachen University, 52072 Germany
[2]GKSS, Geesthacht 21502, Germany.
[3]Stahlwerk Annahütte, Hammerau 83404, Germany
[4]IWT Aachen, 52066 Germany.

ABSTRACT

The failure behaviour of the steel specimens with electron beam welds is analysed in order to understand the mechanisms of crack path deviation, which occurs during stable crack growth. The results can be used as background information for the safety assessment of flawed steel components. The deviation of the crack from the weld into the base metal reduces the risk of sudden load drop occurrence (pop-in's), since the base metal hardly contains brittle zones in contrast to the heterogeneous weld seam. Therefore, it is assumed that the crack path deviation increases the component's resistance to fracture. The crack growth is numerically simulated in fracture mechanic specimens by applying the damage model of GTN (Gurson-Tvergaard-Needleman), which requires the identification of the specific parameters both for the base and weld materials. The metallographical analysis provides the first parameter, the initial void volume fraction f_0, which represents a micromechanical feature. The critical damage parameter f_c is determined from the calculations on the axisymmetric cell model in dependence of the different stress triaxialities. Further parameters, such as element size and damage acceleration factor κ, result from the adaptation of the numerical to the experimental results. For this purpose tests are carried out on the notched round tensile and fracture mechanic specimens under quasistatic loading and compared to the numerical calculations. Once the parameters are determined, they can be used for damage process simulation in specimens with different configurations. The simulation of the crack path deviation is achieved by varying the distance between the fusion line and crack, which is located in the weld seam. The first crack is initiated at the fatigue crack tip in the weld seam. With increasing loading a second crack appears at the fusion line in the base metal due to the high stress triaxiality and the development of plastic zones. In the further process path deviations of both cracks lead to the their coalescence.

1 INTRODUCTION

Every year the power beam welding methods become more important, since they are used for the joining of thick-walled steel components. Power beam welds, such as laser and electron beam welds, have technical and economic advantages in comparison to the conventional welds. The accurate focussing of a laser or electron beam makes possible the application of a high amount of power on very small areas. Due to a reduced heat input, narrow seams and small heat affected zones can be achieved. The following are properties of power beam welds: *overmatching* (higher strength of the weld metal in comparison to the base metal, $M_F>1$) and *crack path deviation*, which depends on the mismatch factor M_F and the weld seam width H. The mismatch factor M_F is defined as ratio between base and weld metal yield strength. Previous experimental results have shown the influence of specimen thickness on the run of the crack [1], [2]. According to these results, it is assumed that crack path deviation can be related to the constraint (development of the local stress fields). For higher loads the constraint decreases at the crack tip, whereas, at the same time, it increases in the bordering base metal. Furthermore, the concentration of the plastic deformation is observed in the base metal [3]. Due to these results, the tendency for the crack path deviation increases with higher loads.

In order to obtain information about the mechanical behaviour during the crack path deviation, it is necessary to integrate material damage into the numerical calculation for the simulation of any ductile crack growth. The damage models describe the interaction between loading and microstructural material damage. Ductile crack initiation is reached if a critical damage value is exceeded.

A phenomenological approach to describe the coalescence of voids due to the damage development is introduced in the model of GTN (Gurson-Tvergaard-Needleman) [4]. In this model the damage can be quantified by using the damage variable f* as a function of the void volume fraction f:

$$f^* = \begin{cases} f & f \le f_c \\ f_c + \kappa(f - f_c) & f_c < f \le f_f \end{cases} \quad \text{with } \kappa = \frac{f_u^* - f_c}{f_f - f_c}$$

In the unloaded state, f is equal to the initial porosity f_0. The critical void volume fraction f_c is reached at the beginning of the void coalescence. The specific void volume fraction f_f corresponds to the occurrence of the macroscopic crack. In this case the damage variable f* reaches its maximum value f_u*.

Since the determination of the parameters is relatively intensive, the investigation is carried out only for one steel material (Grade EMZ355) with electron beam weld (EBW).

2 IDENTIFICATION OF THE DAMAGE PARAMETERS

1.1 Cell model calculation

The parameter f_c can be obtained by means of calculations on the axisymmetric unit cells, which are loaded with different stress triaxialities. The cell model calculation merely requires Young's modulus, yield strength, hardening behaviour of the matrix material, and initial porosity f_0. In order to determine f_0, the microstructural investigations of the polished grinding are conducted with microscopy (s. Fig. 1 a)).

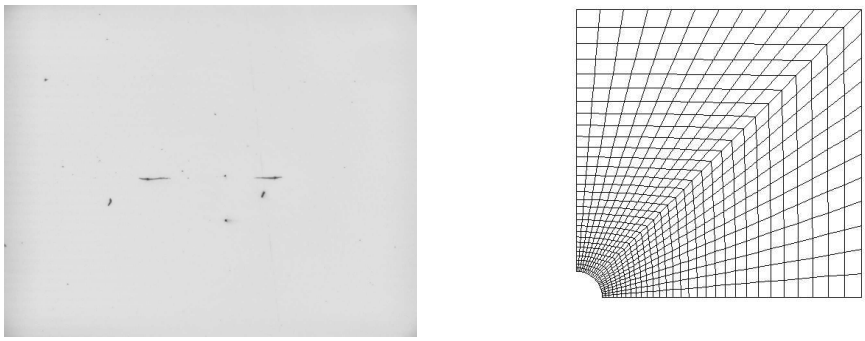

a) b)

Figure 1: a) Base metal: Cut out from the cauterised grinding, b) Undeformed mesh of the cell

The dark emerging objects can be interpreted both as inclusions and voids. The specific inclusions and dispersoids already become detached from the surrounding material in the early phase of plastic deformation. Therefore, they can be regarded as initial voids. The size of these particles ranges from 1 to 8µm. They also have particular morphological constitution and chemical

consistency (e.g. MnS-inclusions). All other inclusions break before they can disperse from the matrix and therefore, must be identified separately from the voids. The present material EMZ 355 contains MnS-inclusions. Their area fraction averages 0.05% and is determined from grinding pictures, at a magnification level of 200. Thus, the initial porosity f_0 is 0.05% and can be used for the cell model calculation. The cell model describes the continuum with periodically arranged cylindrical unit cells and spherical voids [5]. Fig. 1 b) shows an axisymmetric FE model of non-deformed unit cell for f_0=0.0005. The unit cell is based on the following properties:

- Homogeneous displacement is applied along the free boundaries, in order to provide the compatibility of boundaries towards adjacent unit cells.
- The outside edges are loaded with the load ratio, which corresponds to the triaxiality quotient.
- The reduction of the system load capacity is connected with the drop of the load proportionality factor, which corresponds to the principal stress in axial direction.
- In the radial strain versus effective strain diagram, the collapse of the cell is indicated by the point in the radial strain versus effective strain diagram , at which the radial strain no longer increases.

The results of the cell model calculation are presented in the Fig. 2. The critical void volume fraction f_c of 0.026 is graphically determined and shows almost no dependency on the stress triaxiality.

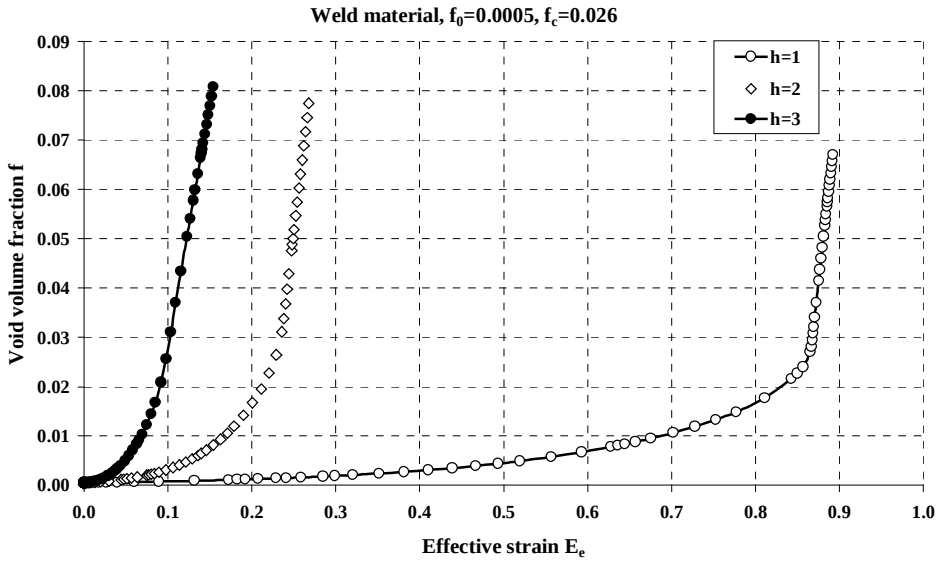

Figure 2: The void volume fraction development for 3 different stress triaxialities h

1.2 Notched round specimen

The determination of the further parameters requires the combination of experimental and numerical results. At first, tensile tests are carried out on notched round specimens with a total length of 96 mm and initial diameter of 8 mm. Two different notch geometries are investigated for homogeneous base metal specimens as well as for specimens with EBW, whereby notch radius ρ and depth t are varied. As an input for the FE-analysis, the flow curves of base and weld materials are obtained from tensile tests on the smooth round specimen at room temperature (microtensile tests for weld material). A mismatch factor of about 1.3 is calculated as the ratio between yield

strength of 388 MPa for the base metal and of 495 MPa for the weld metal. The resulting load versus diameter reduction curves from the tensile tests are then compared with corresponding curves, which are simulated with FE-analysis (s. Fig 4). The element type used is a 2D solid element for axisymmteric stress state. Due to the double symmetry, only a quarter of the specimen needs to be meshed.

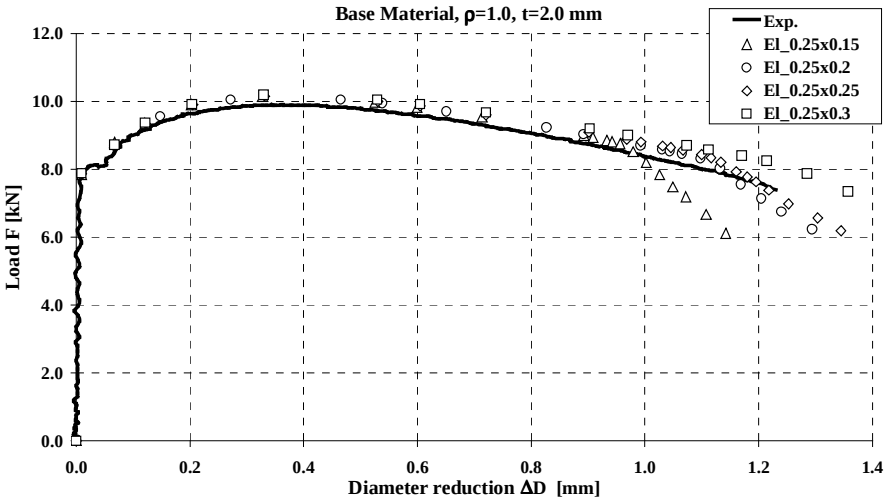

Figure 4: Load versus reduction of diameter of the tensile specimen

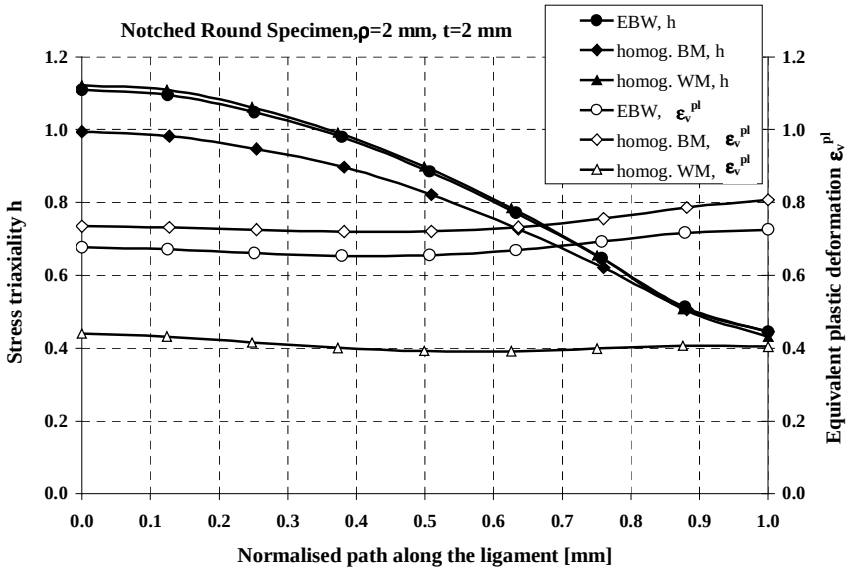

Figure 5: h and ε_v^{pl} along the ligament for $f^*=f_c$

In Figure 4, element height is varied, whereas element width is held constantly at 0.25 mm. With the reduction of element height, the occurrence of the load drop is moved towards smaller diameter reduction values. On the other hand the variation of element width shows no effect on

beginning of the load drop. Element width is set at 0.2 mm and the element height at 0.25 mm for the base metal and 0.15 mm for the weld metal taking into consideration the best correspondence between experimental and numerical results. Maximum load increases and fracture strain becomes smaller with decreasing notch radius, which determines the level of the stress triaxiality.

Figure 5 shows the development of stress triaxiality h and equivalent plastic strain ε_v^{pl} along the ligament of the notched tensile specimen dependent on the material configuration, for the moment when the critical porosity is reached in the centre element of tensile specimen. The difference in the stress triaxiality level between the homogeneous weld metal and the overmatching EBW is very small compared to the plastic deformation, which is distinctly lower for the weld metal. While the plastic zone increases at the notch of the specimen for both the base metal and the weld joint, the plastic deformation is slightly higher at the centre of the specimen for the homogeneous weld metal.

3 THE APPLYING OF THE DAMAGE MODEL ON THE FRACTURE TOUGHNESS SPECIMENS

The determined parameter sets of the damage model are used for the crack growth simulation in specimens with different geometries (CT and SENB specimens) by means of FE program ABAQUS [6]. The objective is to specify the conditions quantitatively, through which crack path deviation occurs. Due to the symmetry a quarter of the specimen is generated with the 3D solid elements (8 nodes). At first, the initial crack is located in the centre of the 3 mm wide weld seam. Although, no crack path deviation is simulated with this crack configuration, the experimental and numerical results correlate well, considering crack initiation and crack growth till maximum load. Afterwards, the difference increases between the experiments and FEA, which can be presumably ascribed to beginning of crack path deviation. Since tested specimens always contain asymmetry with respect to crack location in the weld seam, the crack is moved towards the fusion line by 0.3 mm. In this case, a half of the specimen is regarded. The first crack (crack 1) initiates, when f exceeds f_f in the element at the initial crack tip. In the 2D model (plane strain) of the CT specimen, the first crack extends to 2 mm length, before the second crack (crack 2) emerges at the fusion line on the base metal side. The second crack initiation affects 5 elements, 2.4 mm away from the initial crack tip. Starting from both cracks at the same time, crack path deviation eventually leads to the coalescence of both cracks (s. Fig. 6).

The distribution of stress triaxiality and plastic deformation at the start of crack path deviation

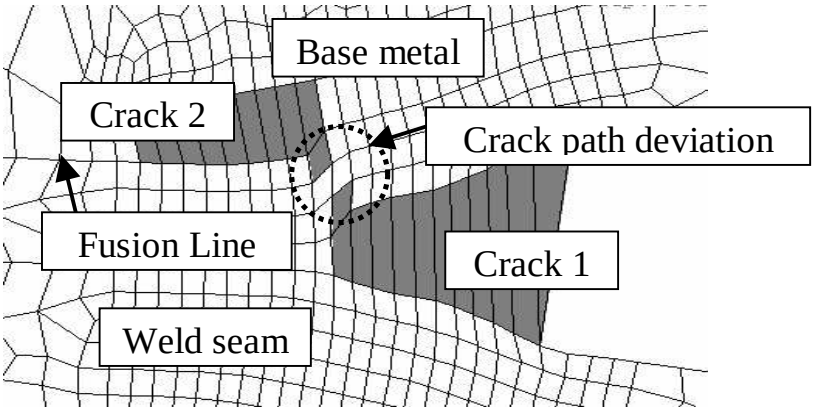

Figure 6: The crack path deviation in the 0.5 CT specimen (2D plane strain calculation)

is presented in the Fig. 7. Due to the development of the second crack in two directions, the stress triaxiality reaches two maxima, which exceed the value of 1. The third maximum of h for the second crack corresponds to the occurrence of crack path deviation, 2 mm away from the initial crack. At this distance, the plastic deformation ε_v^{pl} is a maximum for first, as well as for second crack.

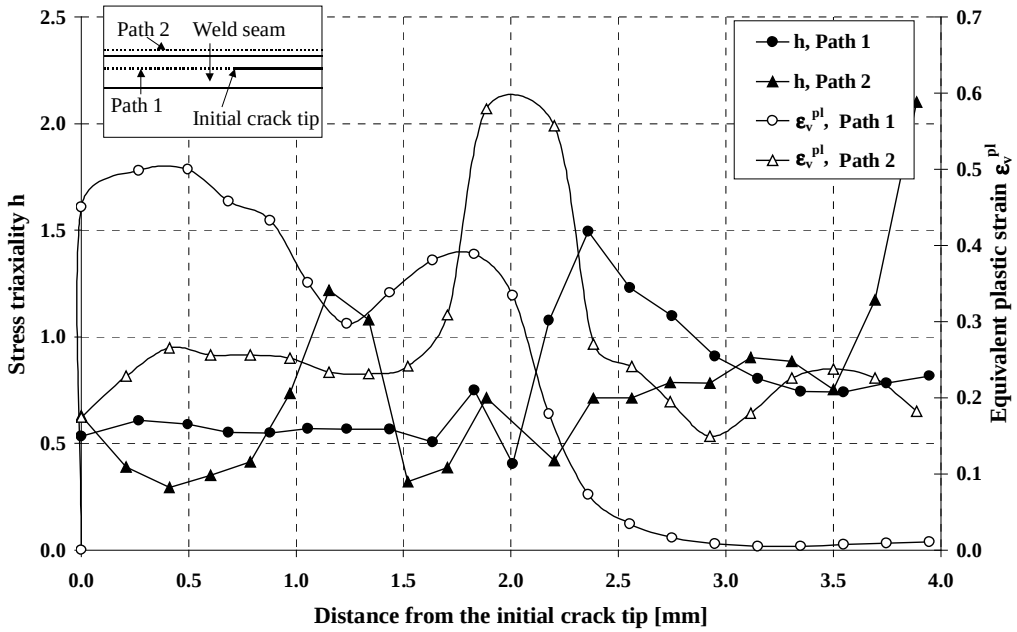

Figure 7: Distribution of h and ε_v^{pl} in CT at the beginning of crack path deviation

4 ACKNOWLEDGEMENTS

This contribution is based on the work done within a project funded by the Deutsche Forschungsgemeinschaft (DFG) (contract No. DA 85/80-2). The authors would like to thank the DFG for its support.

REFERENCES

1. Koçak, M.; Çam, G.; Kim, Y.-J., dos Santos, J. F. (1998) Mechanical and Fracture Properties of Laser Beam Welded Joints, IIW Doc. XV-996-98, 5th Int. Conf. on Trends in Welding Research, June 1-5, Pine Mountain, GA, USA
2. Insfran, A. C. (1999). PhD Thesis, University of Technology Hamburg-Harburg, Germany
3. J. Heyer, P. Langenberg, W. Dahl, Untersuchung von Rissspitzenspannungsfeldern in angerissenen Stahlbauteilen mit Strahlschweißverbindungen mittels FEM, DVM-Bericht 234, Tagungsband zur 34. Tagung des DVM-AK "Bruchvorgänge", 19./20.02.2002,
4. G. Bernauer, W. Brocks, U. Mühlich, D. Steglich, M. Werwer, Hinweise zur Anwendung des des Gurson-Tvergaard-Needleman-Modells, Technical Note GKSS/WMG/99/10 – interner Bericht, GKSS Forschungszentrum, Geesthacht, 1999
5. Eberle, A.; Klingbeil, D., Durchführung von Zellmodellrechnungen mit dem FE-Programm ABAQUS und der Riks_methode, BAM-V.31 Bericht 96/1
6. ABAQUS/Standard User's Manual, Version 6.1 (2000), HKS Inc., Pawtucket, RI, USA